Arch. Metall. Mater. **65** (2020), 3, 1171-1176

DOI: 10.24425/amm.2020.133235

PRASENJIT BISWAS[1], JOYDEEP MAITY[1*]

AN INVESTIGATION ON DIVORCED EUTECTOID GROWTH OF CEMENTITE IN EUTECTOID STEEL

Divorced eutectoid growth of cementite in AISI 1080 steel is investigated as a function of cooling rate for incomplete austenitization-based heat treatment. Furthermore, a fundamental mathematical relationship is established through analytical treatment that correlates divorced eutectoid growth with effective cooling rate and degree of undercooling in view of bulk diffusion controlled growth model. As the cooling rate increases, the divorced eutectoid growth of cementite is gradually ceased. The result predicted by the analytical model closely matches with the experimental result (%Deviation ≤ 7).

Keywords: AISI 1080 steel, incomplete austenitization, cementite, divorced eutectoid growth, analytical model

1. Introduction

Steel is an essential engineering material for the expansion of mankind over several decades. Conventional heat treatment of steel includes complete austenitization based thermal treatments; namely, annealing, normalizing, hardening & tempering etc. Annealing and normalizing processes, in general, are associated with normal eutectoid transformation that involves cooperative growth of ferrite and cementite generating lamellar pearlite structure. There has been a paradigm shift in recent years through the advent of 'incomplete austenitization-based heat treatment' (IAH) [1-4]. This typical approach of heat treatment has brought about novel microstructural changes, accelerated process kinetics and enhanced mechanical properties. One significant effect of IAH is the accelerated lamellar disintegration in AISI 1080 steel; most recently investigated by the research group of present corresponding author [4]. The heat treatment approach involved an incomplete austenitization (through short-span-hold in austenitic region) followed by non-equilibrium air cooling for several cycles. The physical model of the process mechanism proposed for accelerated lamellar disintegration involved: (i) fragmentation of cementite lamella and thickening of lamella (while short-span-hold) followed by (ii) divorced eutectoid growth of cementite particles and (iii) generation of new lamellar faults in remaining cementite lamellae (during non-equilibrium air cooling). On contrary to conventional complete austenitization based heat treatment, incomplete austenitization based heat treatment generates fragmented cementite particles (active nuclei) in austenite matrix while short-span-hold in austenite region. The structure undergoes divorced eutectoid transformation (DET) during subsequent cooling. DET in steel envisages the growth of pre-existing cementite nuclei in austenite matrix with carbon-devoid austenite matrix eventually transforming to α-ferrite. In such case, the cooperative growth of ferrite and cementite does not occur which substantiates the terminology called 'divorced eutectoid' [5-9]. The growth of cementite nuclei is essentially controlled by atomic diffusion [10]. The limited extent of investigations carried out hitherto [10,11] mainly pertain to the growth of cementite particles on isothermal holding below lower critical temperature (A_1) for conventional spheroidizing annealing process. Often the complex modeling approaches (such as multiphase-field model) have been adopted to ascertain the evolved microstructure [11]. However, on advent of IAH and subsequent proposition of physical model [4], a detailed analysis of the divorced eutectoid growth of cementite particles during continuous cooling (instead of isothermal holding) is of utmost necessity for understanding the process mechanism and consequent application in real practice. Accordingly, in the present research work, the divorced eutectoid growth of cementite particles during IAH has been critically investigated in AISI 1080 steel as a function of cooling rate through detailed experimentation and analytical treatment. Instead of complex approaches, the concept of 'effective cooling rate' has been introduced to adopt a conceivable analytical modeling approach that would be effectively utilized in real practice. It is important to note that the primary aim of the present research work is to generate database for the first time pertaining to divorced eutectoid growth

[1] DEPARTMENT OF METALLURGICAL AND MATERIALS ENGINEERING, NATIONAL INSTITUTE OF TECHNOLOGY DURGAPUR, DURGAPUR-713209, WEST BENGAL, INDIA

* Corresponding author: joydeep_maity@yahoo.co.in

of cementite occurring during incomplete austenitization based heat treatment. While this stems the prime novelty, as a secondary approach, a simple, easily conceivable analytical model is approached to support the experimental data.

2. Experimental procedure

The starting material was an annealed AISI 1080 steel (eutectoid steel) possessing a chemical composition: 0.79 mass% C, 0.73 mass% Mn, 0.07 mass% Ni, 0.33 mass% Si, 0.10 mass% Cr, balance Fe. With regard to this chemical composition, as per standard literature [12], the A_1 temperature of this steel was calculated as:

$$A_1 = 723 - 20.7 \times (\text{mass\%Mn}) - 6.9 \times (\text{mass\%Ni}) + \\ + 29.1 \times (\text{mass\%Si}) + 16.9 \times (\text{mass\%Cr}) = \\ = 718.7^{\circ}\text{C} \ (991.7 \text{ K}).$$

Small cubic specimens (with 10 mm edge length) of this steel was held in an electric resistance furnace (temperature control accuracy = ±5°C) at a temperature of 775°C (1048 K) (above the A_1 temperature) for 6 minutes (short duration) so as to cause incomplete austenitization; thereby evolving a microstructure consisting of small fragmented cementite particles (active nuclei) in austenite matrix. This was followed by: (i) ice-brine quenching (to preserve active nucleus); and (ii) cooling in air at different rates (to study divorced eutectoid growth of active nucleus). The detailed heat treatment processes and corresponding specimen codes are summarized in Table 1.

TABLE 1

Specimen code with regard to heat treatment schedule

Specimen code	Heat treatment schedule	Purpose
Q	Short-span-hold (6 min) at 775°C (1048 K) followed by ice-brine quenching	To study initial undissolved fragmented cementite particles (active nucleus)
SA	Short-span-hold (6 min) at 775°C (1048 K) followed by still air cooling	To study cementite particles after divorced eutectoid growth under different rates of cooling
FA1	Short-span-hold (6 min) at 775°C (1048 K) followed by forced air cooling at an air flow rate of 8.7 m^3h^{-1}	
FA2	Short-span-hold (6 min) at 775°C (1048 K) followed by forced air cooling at an air flow rate of 38.4 m^3h^{-1}	
FA3	Short-span-hold (6 min) at 775°C (1048 K) followed by forced air cooling at an air flow rate of 78 m^3h^{-1}	

A digital thermometer (CIE, Model-305, Taiwan) consisting of a K-type thermocouple connected to a digital temperature recorder was used to record the temperature-time data during air cooling at different rates. Metallographic specimens were prepared out of the samples subjected to necessary heat treatment processes by the standard technique of polishing followed by etching in 2% Nital. These specimens were subsequently studied in Field Emission Scanning Electron Microscope (FESEM, Model: SIGMA, Zeiss, Germany), primarily to reveal cementite particle size in divorced eutectoid region. The size of an isolated cementite particle was measured from high magnification FESEM images (considering 20 image frames) as the diameter of a circle possessing an area equal to the area covered by the particle in two-dimensional image. Besides, selected specimens, in the form of thin foils, were studied under high resolution transmission electron microscope (HRTEM, Model: JEM-2100, JEOL, Japan).

3. Results and discussion

3.1 Analysis of Cooling

The experimentally determined cooling curves superimposed on the continuous cooling transformation (CCT) diagram [13] of AISI 1080 steel for different rates of air cooling are shown in Figure 1. Significant data have been obtained from Figure 1 in order to calculate effective cooling rate (r) for different cooling conditions. This is given in Table 2.

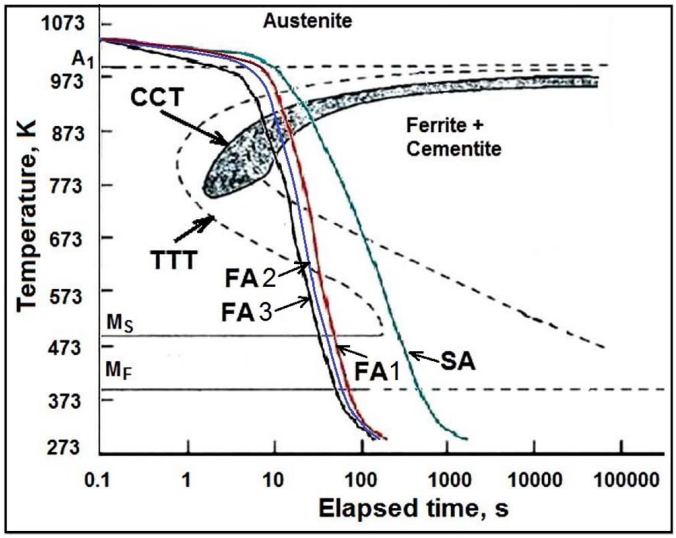

Fig. 1. Cooling curves superimposed on the CCT diagram of AISI 1080 Steel

In the above calculations it is assumed that, during cooling, aided by the presence of active nucleus, divorced eutectoid transformation starts immediately at A_1 temperature without any incubation period (i.e., $T_S = A_1$). However, it achieves completion at a temperature and time similar to normal eutectoid transformation.

3.2. Divorced eutectoid growth

The representative high magnification FESEM micrographs revealing cementite particle size in divorced eutectoid region

TABLE 2

Calculation for effective cooling rate (r)

Specimen code	T_S (A_1), K	T_f, K	$T_{av} = (T_s + T_f)/2$, K	ΔT_{av} ($A_1 - T_{av}$), K	t_1, s	t_{av}, s	Δt_{av} ($t_{av} - t_1$), s	r ($\Delta T_{av}/\Delta t_{av}$), K s^{-1}
SA	991.7	887.3	939.5	52.2	10.28	17.59	7.31	7.14
FA1	991.7	853.8	922.75	68.95	7.77	13.51	5.74	12.01
FA2	991.7	842.2	916.95	74.75	5.53	8.96	3.43	21.79
FA3	991.7	813	902.35	89.35	4.32	6.75	2.43	36.77

The terms used in Table 2 are described below:

T_S – Divorced eutectoid transformation-start temperature (assumed to be equal to A_1 = 718.7°C (991.7 K)),

T_f – Divorced eutectoid transformation-finish temperature (assumed to be equal to the pearlitic transformation-finish temperature),

T_{av} – Average transformation temperature, given by $(T_S + T_f)/2$,

ΔT_{av} – Average degree of undercooling = $(A_1 - T_{av})$,

t_1 – Transformation-start time corresponding to $T_S(A_1)$,

t_{av} – Transformation time corresponding to T_{av},

Δt_{av} – Time interval corresponding to $\Delta T_{av} = (t_{av} - t_1)$,

r – Effective cooling rate = $\Delta T_{av}/\Delta t_{av}$.

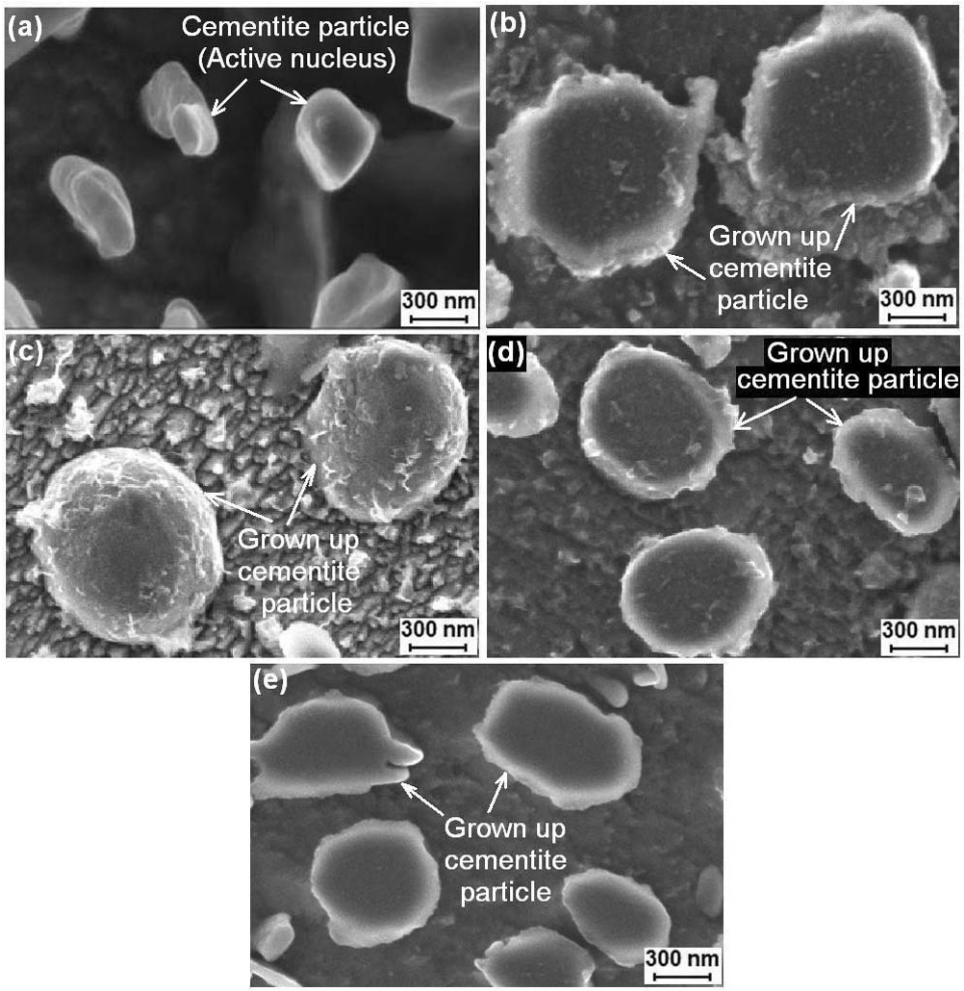

Fig. 2. FESEM micrographs of heat treated specimens representing cementite particle size in divorced eutectoid region: (a) Q, (b) SA, (c) FA1, (d) FA2, (e) FA3

are shown in Figure 2(a)-(e). The measured particle sizes and divorced eutectoid growth for different air cooling rates are presented in Table 3.

Figure 2(a) represents the cementite particle size in ice-brine quenched specimen (i.e. the size of active nucleus denoted as D_i) which is quite small (466±22 nm). The interparticle distance (λ) between these cementite particles (active nucleus) was measured as 800±75 nm. Figures 2(b) to (e) corroborate the cementite particle size after divorced eutectoid growth (denoted as D_f) under different rates of air cooling. The divorced eutectoid growth ($\Delta D = D_f - D_i$) of cementite particles is gradually ceased with faster rate of cooling (Table 3). Furthermore, HR-TEM image of a typical cementite particle subjected to divorced eutectoid growth under still air cooling and its selected area electron diffraction pattern (SADP) are shown in Figure 3(a) and (b).

TABLE 3

Experimentally determined divorced eutectoid growth

Code of quenched specimen	Cementite particle (active nucleus) size in quenched specimen (D_i), nm (mean ± standard deviation)	Codes of specimens undergone divorced eutectoid transformation	Sizes of grown up cementite particles (D_f), nm (mean ± standard deviation)	Divorced eutectoid growth of cementite particles ($\Delta D = D_f - D_i$), nm
Q	466 ± 22	SA	1127 ± 21	661
		FA1	1024 ± 29	558
		FA2	838 ± 35	372
		FA3	770 ± 32	304

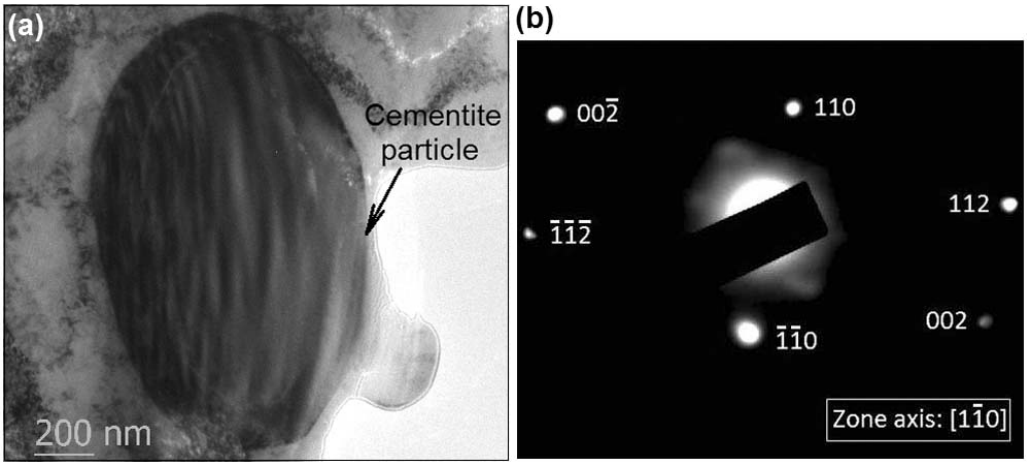

Fig. 3. Characterization of a cementite particle subjected to divorced eutectoid growth under still air cooling (SA) in view of (a) HRTEM bright field image, and (b) its SADP

3.3. Analytical treatment

The primary aim of the present research work is to generate database for the first time pertaining to divorced eutectoid growth of cementite occurring during incomplete austenitization based heat treatment. However, as a secondary approach, a simple, easily conceivable analytical model is approached to support the experimental data. In case of incomplete austenitization based heat treatment; at the onset of cooling, pre-existing cementite nuclei are already present in austenite matrix. Therefore, divorced eutectoid transformation would have three kinetic steps; namely, (i) atomic diffusion from bulk austenite to the vicinity of pre-existing cementite nuclei, (ii) atomic migration across interface, and (iii) concurrent polymorphic transformation of austenite-to-ferrite. The first step (bulk diffusion) is expected to be the rate controlling step which is taken into account in the present analytical model. Subsequent atomic migration across interface and polymorphic transformation of austenite-to-ferrite are much faster processes and therefore, cannot be the rate controlling step [14].

Following Fick's first law of diffusion and invoking the Zener approximation of a linearized concentration profile [14], the diffusion flux represented in terms of velocity (v_c) of solute (carbon) atom diffusing from bulk austenite to the vicinity of cementite spheroid can be expressed as:

$$v_c = D_C\left(\frac{X_b - X_s}{\beta\lambda}\right) \tag{1}$$

Where, D_C is the diffusion coefficient of carbon in austenite; X_b, the mass fraction of carbon in bulk austenite; X_s, the mass fraction of carbon in the vicinity of cementite spheroid; $\beta\lambda$, the mean diffusion distance of carbon, which is considered as a fraction (β) of mean interparticle distance (λ). It is important to note that, representation of concentration in terms of dimensionless mass fraction (X) instead of mass per unit volume, eventually represents diffusion flux in terms of velocity (in ms^{-1} unit).

Now, the volume (V_c) of carbon diffuses in unit time (volumetric flux) for each cementite spheroid growth,

$$V_c = 4\pi\left(\frac{D_i}{2}\right)^2 v_c = \pi D_i^2 v_c \tag{2}$$

Therefore, the mass of carbon diffuses for each cementite spheroid growth,

$$m_c = V_c\rho_c\Delta t_{av} = \pi\rho_c D_i^2 v_c\Delta t_{av} \tag{3}$$

Putting the value of v_c from Eq. (1),

$$m_c = \pi D_i^2\rho_c D_c\left(\frac{X_b - X_s}{\beta\lambda}\right)\Delta t_{av} \tag{4}$$

Where ρ_c is the density of carbon.

This would be equal to the mass of carbon in grown up part of each spheroid. Accordingly,

$$m_c = f_c \rho_{cm} \left[\frac{4}{3}\pi \left(\frac{D_f}{2} \right)^3 - \frac{4}{3}\pi \left(\frac{D_i}{2} \right)^3 \right]$$

$$m_c = \frac{\pi}{6} f_c \rho_{cm} [{D_f}^3 - {D_i}^3] \quad (5)$$

Where, ρ_{cm} is the density of cementite; f_c, the mass fraction of carbon in cementite.

Therefore, as per Equation (4) and (5),

$$\pi {D_i}^2 \rho_c D_c \left(\frac{X_b - X_s}{\beta \lambda} \right) \Delta t_{av} = \frac{\pi}{6} f_c \rho_{cm} \left[{D_f}^3 - {D_i}^3 \right]$$

$${D_f}^3 - {D_i}^3 = \frac{6{D_i}^2 \rho_c D_c}{f_c \rho_{cm}} \left(\frac{X_b - X_s}{\beta \lambda} \right) \Delta t_{av}$$

$$D_f = \left[\frac{6{D_i}^2 \rho_c D_c}{f_c \rho_{cm}} \left(\frac{X_b - X_s}{\beta \lambda} \right) \Delta t_{av} + {D_i}^3 \right]^{\frac{1}{3}}$$

$$\Delta D = D_f - D_i = \left[\frac{6{D_i}^2 \rho_c D_c}{f_c \rho_{cm}} \left(\frac{X_b - X_s}{\beta \lambda} \right) \Delta t_{av} + {D_i}^3 \right]^{\frac{1}{3}} - D_i$$

Since $\Delta t_{av} = \frac{\Delta T_{av}}{r}$, final expression of divorced eutectoid growth (ΔD) of cementite particles in AISI 1080 steel may be represented as:

$$\Delta D = \left[\frac{6{D_i}^2 \rho_c D_c}{f_c \rho_{cm}} \left(\frac{X_b - X_s}{\beta \lambda} \right) \frac{\Delta T_{av}}{r} + {D_i}^3 \right]^{\frac{1}{3}} - D_i \quad (6)$$

Now, X_b can be expressed as: $X_b = \alpha f_c$, where α is the fraction of cementite lamella dissolved in austenite while holding steel specimen at 775°C for 6 minutes. α is experimentally found out as 0.44 from the microstructure analysis in terms of the ratio of the area fraction occupied by fragmented cementite lamellae in the steel specimen ice brine quenched from 775°C after holding for 6 minutes to the area fraction occupied by cementite lamellae in pearlite in as received steel specimen. f_c, the mass fraction of carbon in cementite is known to be 0.0667. Accordingly, X_b = 0.029348. X_s may be considered as 0.00025 which is the maximum solubility (expressed in terms of mass fraction) of carbon in α-iron at A_1 temperature (991.7 K) on the onset of divorced eutectoid growth, since in concurrence to the divorced eutectoid growth of a cementite particle the adjacent matrix transforms to α-ferrite. The diffusion coefficient of carbon in austenite (D_C) can be calculated from familiar relationship: $D_C = D_0 e^{-Q/RT}$. The values of activation energy (Q) and frequency factor (D_0) are obtained from standard literature [15] as 157×10^3 J mol^{-1} and 0.7×10^{-4} m^2 s^{-1}, respectively. Accordingly, at A_1 temperature (T = 991.7 K), on the onset of divorced eutectoid growth, D_C is calculated as 3.76118×10^{-13} m^2 s^{-1}. The interparticle distance (λ) is experimentally measured from FESEM image (Figure 2(a)) as 800×10^{-9} m (as discussed earlier). Furthermore, the value of molar gas constant (R) is known to be as 8.314 J mol^{-1} K^{-1} [15]. An analytical derivation requires necessary approximations and associated effective values to consider for obtaining an easily conceivable expression (Eq. (6)) applicable in real practice. Accordingly, effective value of diffusion coefficient is chosen on onset of divorced eutectoid transformation (at A_1 temperature). Furthermore, under air cooling conditions transformation achieves completion above nose temperature, thereby envisaging major diffusion to occur near A_1 temperature. Such considerations of effective diffusion coefficient are readily available in standard literature [15]. Again, it is a plausible approach to consider the value of β as 0.5. This realizes the bulk diffusion to occur from midway between two neighbouring cementite particles, as also indicated in literature [14]. The value of D_i is experimentally measured as 466×10^{-9} m (as discussed earlier). Furthermore, as per standard literature: ρ_c = 2260 Kg m^{-3} [16], ρ_{cm} = 7640 Kg m^{-3} [17]. Accordingly, divorced eutectoid growth (ΔD) can be obtained from Equation (6) developed through analytical model for different ΔT_{av} and r values (as per Table 2) with regard to different cooling conditions. Table 4 shows a comparison between the experimental value (ΔD_{ex}) and predicted value (ΔD_{pr}) of divorced eutectoid growth obtained through analytical treatment (given by Eq. (6)) in terms of %Deviation $\left(\left| \frac{\Delta D_{ex} - \Delta D_{pr}}{\Delta D_{ex}} \right| \times 100 \right)$. The experimental data closely matches with predicted data (%Deviation ≤ 7) authenticating the expression of ΔD (Eq. (6)) obtained through analytical treatment. This is further graphically presented in Figure 4.

The physical interpretation of Eq. (6) can be realized with shorter time available for atomic diffusion that ceases growth (ΔD) in case of faster cooling rate (r). This is quite reasonably supported by experimentation (Figure 2(a)-(e), Table 3). Besides, as exemplified in Eq. (6), more degree of undercooling (ΔT_{av}) would augment growth. Again, it is interesting to note the counteracting effect of r and ΔT_{av}, since faster rate of cooling would lower down the transformation-finish temperature (Table 2). The resultant outcome is the overall arrest in divorced eutectoid growth with increasing cooling rate (Table 3). It is interesting to note that, the divorced eutectoid growth of cementite, primarily occurring through the bulk diffusion of interstitial solute (carbon) under continuous cooling (in still air or forced air), does not replicate isothermal parabolic growth law, often observed during grain growth or growth of oxides. This envisages the unique feature of the new kind of growth expression developed under continuous air cooling. The significance of the analytical expression (Eq. (6)) derived in the present research work stems from obtaining desired cementite particle size under a particular 'effective cooling rate' chosen during incomplete austenitization based heat treatment in real practice. In particular, unlike conventional spheroidizing annealing (involving long duration isothermal holding below A_1 temperature), the cementite particles of submicroscopic sizes in α-ferrite matrix generated through incomplete austenitization based heat treatment have been found to result in simultaneous enhancement in strength and ductility of AISI 1080 steel [18].

Furthermore, with judicious selection of cooling rate (so as to optimize divorced eutectoid growth) a strength level as high as 2 GPa along with reasonable ductility and wear resistance have been achieved in AISI 1080 steel [19,20]. In this regard, this is the first mathematical approach for the quantification of divorced eutectoid growth of cementite in AISI 1080 steel under incomplete austenitization based heat treatment.

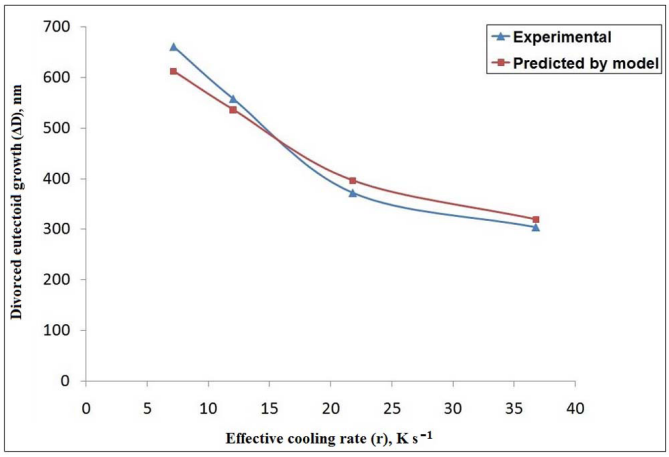

Fig. 4. Divorced eutectoid growth (ΔD) as a function of effective cooling rate (r)

TABLE 4

Comparison between experimental and predicted divorced eutectoid growth values

Specimen code	Experimental ΔD, nm	Predicted ΔD, nm	% Deviation
SA	661	613	7
FA1	558	537	4
FA2	372	397	7
FA3	304	320	5

4. Conclusion

The study of divorced eutectoid growth of cementite through incomplete austenitization (to obtain a microstructure containing active cementite nucleus in austenite matrix) followed by cooling in air at different rates envisages an inverse relationship between growth of cementite particles with effective cooling rate. The mathematical relationship established through analytical treatment also substantiates this inverse relationship of divorced eutectoid growth with effective cooling rate. The experimentally obtained divorced eutectoid growth data closely follow the analytically derived relationship (%Deviation ≤ 7) primarily on the basis of bulk diffusion controlled growth model.

Acknowledgement

Mr. Prasenjit Biswas carried out the main part of experimental work for this investigation under the guidance of Professor Joydeep Maity who conceived and formulated the analytical model of divorced eutectoid growth. No external funding source was utilised for carrying out this research work. The authors are thankful to the Director, National Institute of Technology Durgapur, India, for the necessary administrative support.

REFERENCES

[1] J. Maity, A. Saha, D.K. Mondal, K. Biswas, Phil. Mag. Lett. **93**, 231 (2013).
[2] A. Saha, D.K. Mondal, J. Maity, Mater. Sci. and Eng. A **527**, 4001 (2010).
[3] A. Mishra, C. Mondal, J. Maity, Steel Res. Int. **87**, 424 (2016).
[4] S. Mishra, A. Mishra, B.K. Show, J. Maity, Phil. Mag. Lett. **97**, 140 (2017).
[5] S.L. Gertsman, Research and special projects report, Canadian Department of Mines and Technical Surveys, Otawa 1966.
[6] K. Honda, S. Saito, Journal of the Iron and Steel Institute **102**, 261 (1920).
[7] G.B. Lure, Y.I. Shteinberg, Metal Science and Heat Treatment **11**, 351 (1969).
[8] T. Oyama, O.D. Sherby, J. Wadsworth, B. Walser, Scripta Metallurgica **18**, 799 (1984).
[9] J.H. Whitley, Journal of the Iron and Steel Institute **105**, 339 (1922).
[10] A.S. Pandit, H.K.D.H. Bhadeshia, Proc. R. Soc. A **468**, 2767 (2012).
[11] K. Ankit, R. Mukherjee, B. Nestler, Acta Mater. **97**, 316 (2015).
[12] K.W. Andrews, J. Iron Steel Inst. Jpn. **203**, 721(1965).
[13] M. Ohring, Engineering Materials Science, Academic Press, New York 1995.
[14] P.E.D. Nunzio, Phil. Mag. **98**, 1674 (2018).
[15] V. Raghavan, Materials Science and Engineering: A First Course, Prentice Hall of India Private Limited, New Delhi 1995.
[16] J.F. Shackelford, Introduction to Materials Science for Engineers, Macmillan Publishing Company, New York 1992.
[17] Anon, Iron Carbide Manufacturing Process, International Iron Carbide (LLC) Report, Colorado, USA, November 2011.
[18] S. Mishra, A. Mishra, B.K. Show, J. Maity, Mater. Sci. and Eng. A **688**, 262 (2017).
[19] A. Mishra, C. Mondal, J. Maity, Steel Res. Int. **88**, 1 (2017), (Article number 1600215).
[20] A. Mishra, J. Maity, J. Mater. Eng. Perform. **27**, 398 (2018).